

Performance Evaluation of the Nexalus Liquid Cooled Open Compute Project Cubby

RISE Research Institutes of Sweden

Jeffrey Sarkinen

Jon Summers

2021-10-06

Version 2.1 Draft



Contents

Table of Figures	3
Executive Summary.....	4
Introduction	5
Method	6
Connection to RISE Liquid cooling testbed	6
Flow Meter setup and calibration.....	8
Server Pump Control and Measurement.....	9
Profiling Server fans	9
Data collection	10
Control Methodology.....	10
Results and Analysis.....	12
Conclusion.....	18
References	19

Table of Figures

Figure 1: 2015 ASHRAE thermal guidelines for liquid cooling [1].	5
Figure 2: Experimental setup of the Nexalus cubby of 3 OCP servers at the RISE ICE test and demo Data Center lab in Luleå, Sweden.	6
Figure 3: Photo of the RISE liquid cooling testbed with indications of the hot and cold supplies of water and the connection point for the liquid cooled IT equipment.	7
Figure 4: The picture on the left shows the bleed valve located at the highest point in the system. The picture in the middle shows the server connections to the heat exchanger and the valve used for filling the system. The picture to the right shows the heat exchanger used for the connection to the liquid cooling test bed.	7
Figure 5: Shown on the left is the Arduino frequency counter running in parallel with the PFM3000 frequency counter. The figure shows the results of the flow meter calibration using the Arduino frequency counter.	8
Figure 6: All the components for operating the pump are shown in the picture including the power supply, Arduino frequency counter, micropump control unit, the pump, the DAC and the raspberry pi.	9
Figure 7: Plot of data showing relationship between server fan speed and power. On the right a picture is shown which was taken during the experiment.	10
Figure 8: Measurement and control schematic.	11
Figure 9: Photo showing the 20U air-cooled OCP server (lower) and the 1U direct-to-chip Nexalus cooled OCP server (upper). Note that the water flow and air flow are in opposite directions as indicated and that there are small fans in the upper server to supply air to the DIMMs.	11
Figure 10: 3 OCP server enclosure showing the water and DC power connection points and the channels for the recirculated air over the air-to-liquid heat exchangers.	12
Figure 11: Plots showing the average server thermal power based on the targeted average CPU temperature.	13
Figure 12: Cooling power consumption (water pump and fans for memory) as a function of the targeted CPU temperature.	13
Figure 13: CPU power consumption as a function of the average CPU temperature for the 3 IT workloads.	14
Figure 14: DIMM temperatures as a function of targeted CPU temperatures. Note: DIMM temperatures should stay below 85°C.	14
Figure 15: Total power consumed averaged over the three servers in the cubby for the different coolant supply temperatures as the targeted average CPU temperature is varied.	15
Figure 16: Server thermal power after the CPU thermal output is discounted.	16
Figure 17: Breakdown of average total power consumption for each server between cooling and thermal when the coolant supply is at 30°C.	16
Figure 18: Breakdown of thermal power production and required cooling power overhead as a function of average CPU temperature for 40°C (Left) and 50°C (right).	17
Figure 19: Plots of the return coolant water temperature for the three different workloads and three supply temperatures.	17

Executive Summary

This report provides an independent, systematic and detailed analysis of a Nexalus direct-to-chip liquid cooled arrangement of three 2nd generation Open Compute Project (OCP) servers supplied by Nexalus for assessment, and to be referred to throughout this report as 'Nexalus servers'. The main aim of this study is to determine the behaviour of these OCP Nexalus servers at fixed average CPU temperatures and compare the results against the same specification of server that utilises a standard air-cooled setup in a well-tuned server wind tunnel, with a particular focus on the energy recovery potential of the Nexalus solution.

During our investigations the Nexalus servers were connected to a low pressure drop crossflow heat exchanger so the supply temperature could be accurately controlled. Our analysis used three supply temperatures of 30°C/86°F, 40°C/104°F and 50°C/122°F, and for comparison the same specification air-cooled OCP servers were operated on with a 30°C/86°F air supply temperature, with a neutral drop in air pressure across the servers and their fans.

In all cases the servers were operated at three different workloads, based on a targeted CPU workload namely; 8%, 50% and 75%, to simulate and capture some typical cloud server utilisation levels.

The primary observations of note include the following;

1. The Nexalus solutions across all 3 workloads and servers enabled energy recovery at an average of 93%
2. The Nexalus configuration facilitated the production of thermal energy in the form of 64°C/147.2°F hot water at all workloads, with a 30°C/86°F water supply. This is high quality hot water suitable for immediate use, without the requirement of further intervention to increase temperatures.
3. Rack density is doubled with the Nexalus solution, dropping from 20U to 10U. This is achieved by the removal of the OCP air-cooled heat sinks, which are replaced with direct-to-chip cooling heads.
4. When the Nexalus solution is compared with the air-cooled equivalent servers, the CPU temperature is much cooler vs. the water or air supply temperature, seeing a 15°C/59°F approach versus 25°C/77°F for air at a 50% workload. These cooler operating temperatures result in better CPU performance, while also enabling energy recovery.
5. The high-density Nexalus DIMM configuration of 256GB in their servers resulted in the DIMMS running hotter than in the air-cooled solution. However, the Nexalus solution uses an air to liquid heat exchanger inside the server to transfer the DIMM thermal output into the coolant water loop - an innovative solution that reduces the need for additional cooling outside of the server enclosure.

In conclusion, the results demonstrate important advantages of this new closed loop, direct-to-chip liquid cooling approach by Nexalus. These benefits include the opportunity for cooler CPUs and 90+% energy recovery. This innovative solution, which does not completely rid data centres of their existing form factor, provides a great option for driving data centres forward towards a space where they become energy borrowers rather than just large energy consumers. We look forward to watching Nexalus tackle future server and data centre energy issues, bringing more thermal science and engineering breakthroughs to market.

Introduction

Thermal management of data center servers is very important from the point of view of their operation and their performance. The temperature of the air supply to the front of air-cooled servers is governed by the data center cooling system and the range of temperature and humidity values is mandated to a certain extent by the American Society of Heating, Refrigerating and Air-conditioning Engineers (ASHRAE) Technical Committee 9.9 (TC9.9), which have published guidelines for recommended and allowable air supply characteristics. The server manufacturers are known to warranty their servers to operation in the class of the allowable ranges, namely A1, A2, etc. The increases in the range of operational air temperatures have enabled data centers to reduce their dependence on refrigeration systems and therefore the need to maintain plants that use compressor-based technologies, and thus the need to adhere to the F-Gas regulations. Chilled water systems with free cooling capability still require the use of compressor technologies to overcome external seasonal ambient conditions where refrigeration is required.

Equipment Environment Specifications for Liquid Cooling			
Class	Typical Infrastructure Design		Facility Supply Water Temperature, °C (°F)
	Main Cooling Equipment	Supplemental Cooling Equipment	
W1	Chiller/cooling tower	Water-side economizer	2 to 17 (35.6 to 62.6)
W2			2 to 27 (35.6 to 80.6)
W3	Cooling tower	Chiller	2 to 32 (35.6 to 89.6)
W4	Water-side economizer (with dry-cooler or cooling tower)	N/A	2 to 45 (35.6 to 113)
W5	Building heating system	Cooling tower	>45 (>113)

Figure 1: 2015 ASHRAE thermal guidelines for liquid cooling [1].

Data centers operate all year round and their thermal management is continuously challenged by the requirement to reject the servers' heat during the full range of external ambient conditions without the need for a plant that uses refrigeration or excessive amounts of water (in the case of technologies that employ evaporative and adiabatic cooling). It is also becoming understood that the data center servers of the future will contain integrated circuits that are less thermally tolerant (removing thermal design power limits and addressing dark silicon issues, see IRDS¹ – the roadmap ITRS 2.0 was predicting lower operating temperatures), and with the sustainability requirements of future data centers demanding waste heat recovery, is providing a stronger impetus to adopt what is commonly called *liquid cooling*, where the data center water cooling penetrates the IT space, and the hot microelectronics are connected to a water circuit that harvests the thermal energy and transfers it out of the data center for reuse. Liquid cooling of microelectronics can be achieved using a multitude of approaches, but in all cases the setup requires a liquid (usually water) circuit that enters the Cooling Distribution Unit (CDU) that is proximal to the IT equipment. The temperature of the facility water to the CDU has also been classified by ASHRAE guidelines

¹ <https://irds.ieee.org/>

and can be found in the DataCom Series volume 1, edition 4 on Thermal Guidelines [1], highlighted in Figure 1. The water set points in the experimental results shown and discussed later are governed by the W classes of operation depicted in Figure 1.

Method

Connection to RISE Liquid cooling testbed

The Nexalus server was setup on a bench with instrumentation to track temperature, water flow rate and power consumption as seen in Figure 2. The water connections were connected to a flat plate heat exchanger (Alfa Laval CBH16-13H) which was connected to the RISE liquid cooling testbed, shown in Figure 3. The testbed allows temperature control to the heat exchanger from 20 – 48°C and a variable flow rate between 3-8 l/min. For inlet temperatures to the server below 50°C (ASHRAE guideline class W4 or less in Figure 1) a fixed flow rate of 8 l/min will be used and the temperature will be adjusted. If inlet temperatures above 50°C are desired (for ASHRAE guideline class W5 operation - Figure 1), the flow rate will be reduced accordingly from 8 l/min. In the pipework connecting the server to the heat exchanger, two T-valves were included, one with the purpose of filling the system and the other for releasing air or reducing the pressure in the system.

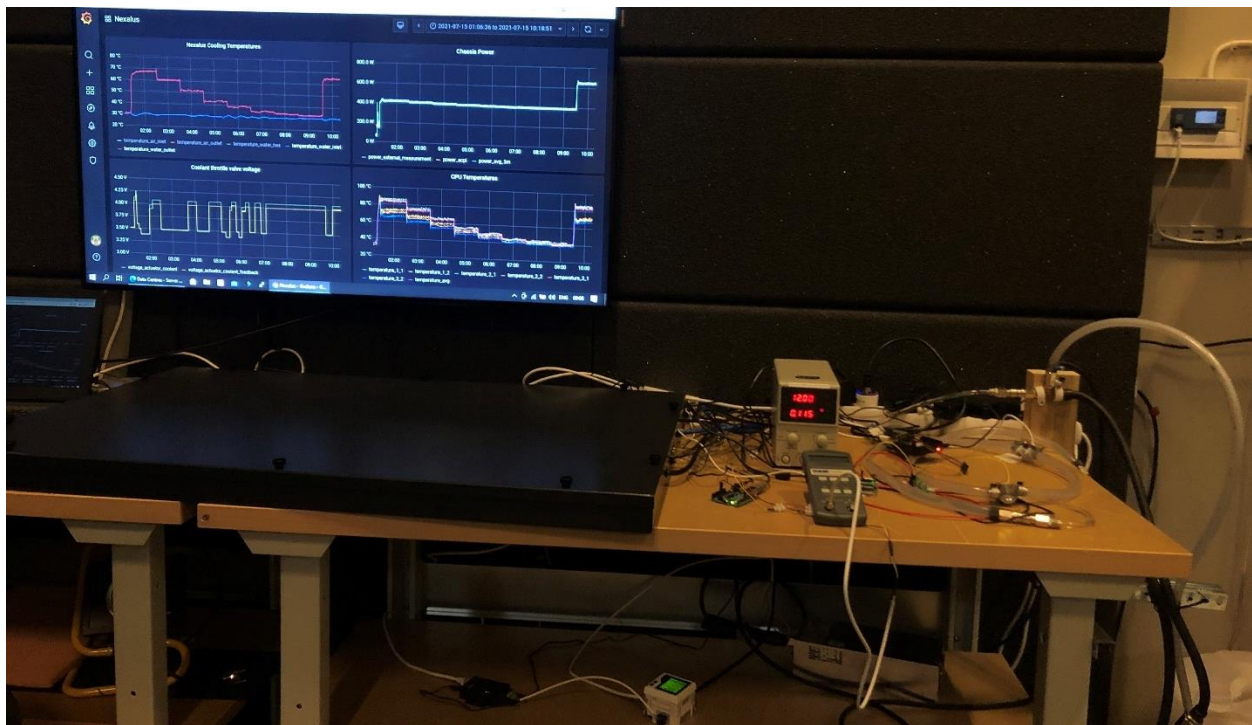


Figure 2: Experimental setup of the Nexalus cubby of 3 OCP servers at the RISE ICE test and demo Data Center lab in Luleå, Sweden

Referring to Figure 3, the RISE ICE test and demo data center liquid cooling test bed is connected to two different water circuits. To the left of the test bed, there is a hot water supply (of 60°C or more) coming from the hot water loop in the facility (shown via the red arrow) and to the right there is a chilled water loop (shown by the blue arrow). The water circuits are configured so that the hot water (which can be throttled) is supplied to the heat exchanger, which is cooled down by the chilled water loop from the top heat exchanger and this can be cooled down to a desired temperature that is based to a second heat

exchanger (directly below the first) to supply the water loop to the IT equipment at the desired temperature. For the purpose of the Nexus liquid cooled OCP cubby, the connection loop from the liquid cooling test bed will employ one further heat exchanger, shown in the middle and right photos of Figure 4, so that the pressure drop on the liquid cooling loop that includes the 3 Nexus liquid cooled OCP servers is reduced as much as possible.

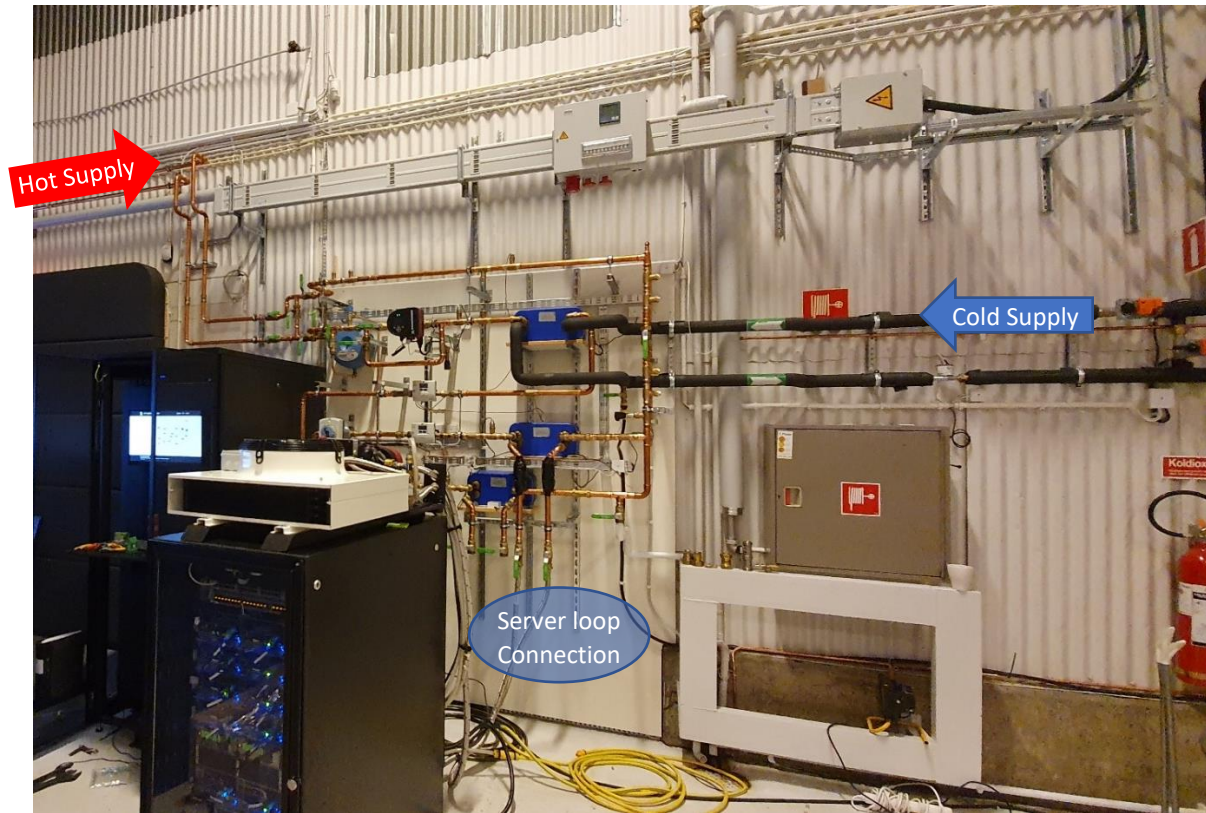


Figure 3: Photo of the RISE liquid cooling testbed with indications of the hot and cold supplies of water and the connection point for the liquid cooled IT equipment.

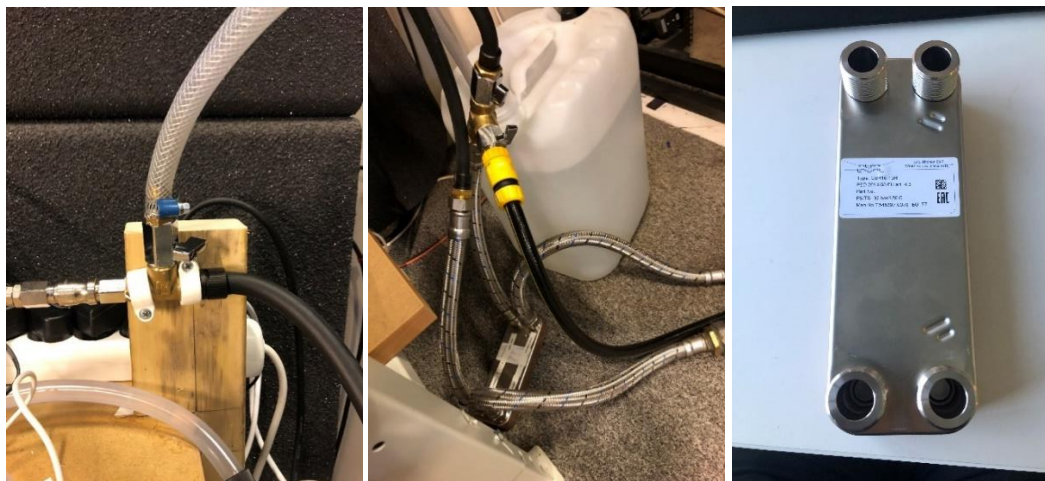


Figure 4: The picture on the left shows the bleed valve located at the highest point in the system. The picture in the middle shows the server connections to the heat exchanger and the valve used for filling the system. The picture to the right shows the heat exchanger used for the connection to the liquid cooling test bed.

Once the connections were complete the system was then flushed using tap water to force all the air out of the system, see the left photo in Figure 4. The pump was power cycled several times during this process to remove any captured air. During this flushing process, the flow meter was also calibrated since an open loop system with a vessel is needed to measure the amount of water. On completion of the calibration procedure, the loop was closed, and the pump was power cycled several more times and any residual air was released through the bleed valve.

Flow Meter setup and calibration

A flow meter (RS PRO 511-4722) with a range of 0.6 to 10 l/min was used to measure the water flow rate to the server. The flow meter generates a pulse with a frequency that corresponds to the flow rate. A frequency counter was provided by Nexalus (PFM3000) which was lacking an output to enable monitoring using the RISE data collection system. To solve this issue, RISE constructed a bespoke frequency counter using an Arduino UNO with the FreqMeasure² library that provides an RS-232 serial output via the USB port, as shown in Figure 5. The Arduino frequency counter was verified by taking 3 measurements at 3 different flow rates with a 10s average and comparing the outputs against the PFM3000 with the 10s filter enabled. The results showed that the devices measured to within 0.2% of each other. The Arduino frequency meter was then connected to a raspberry pi and sampled by the data collection system at a rate of 5s intervals. The reading obtained by the Arduino frequency meter averages the frequency readings over a 1 second time duration.

The flow meter was then calibrated by averaging the frequency readings from the Arduino meter while filling a bucket with water for a fixed time. The water was then weighed using a scale and the flow rate was calculated. A total of 4 flow rates were tested and each test was run to obtain approximately 4-5 liters of water. The results can be seen in the plot in Figure 5 as a linear relationship between frequency and flowrate.

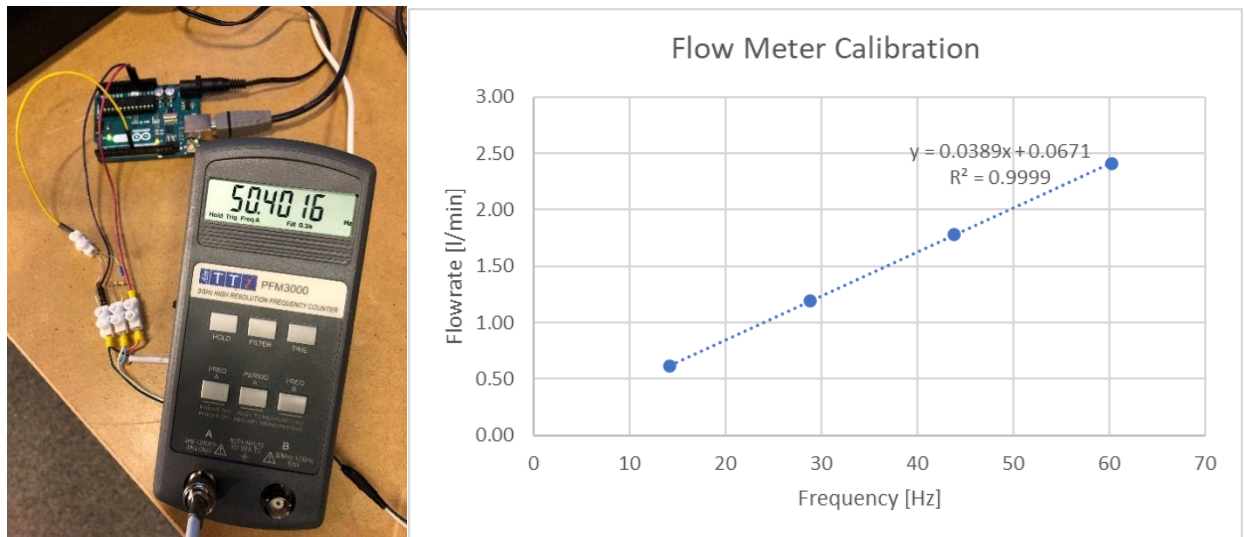


Figure 5: Shown on the left is the Arduino frequency counter running in parallel with the PFM3000 frequency counter. The figure shows the results of the flow meter calibration using the Arduino frequency counter.

² <https://github.com/PaulStoffregen/FreqMeasure>

Server Pump Control and Measurement

To enable monitoring of the pump power in the RISE data collection system, a new power supply was procured as the one provided by Nexalus lacked the RS232 data connection. The power supply was then connected with a RS232 to USB cable to the raspberry pi to read both the voltage and current to the pump using python.

The pump was controlled using a micropump control unit (TCS EQi-MG2) which allows pump control using a 0-5V signal while keeping the pump supply voltage fixed at 12V. The 0-5V signal was provided by a digital to analog convertor (DAC) (MCP 4725) which was connected to the raspberry pi. The voltage to the pump was used to alter the flow rate to regulate the CPU temperature on the servers described in the control system section below.

The micropump control unit also provided an output for the pump RPM which was monitored with another Arduino frequency counter. This was useful for estimating flow at low flow rates. All the components for controlling and monitoring the pump are shown in Figure 6.

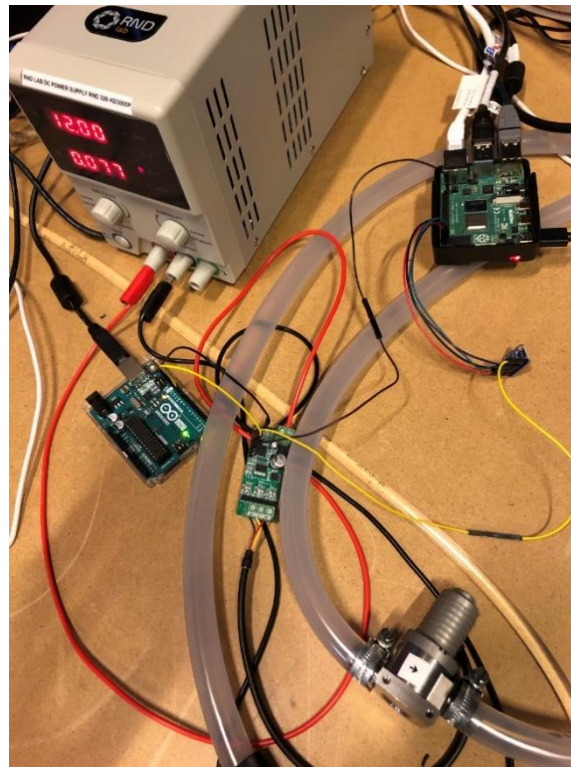


Figure 6: All the components for operating the pump are shown in the picture including the power supply, Arduino frequency counter, micropump control unit, the pump, the DAC and the raspberry pi.

Profiling Server fans

To gain a full understanding of the cooling power used in the Nexalus server arrangement, the DIMM cooling fans (SAN ACE 40) were profiled to obtain a relationship between their fan speed and power consumption. This was done by measuring the fan speed as well as the voltage and current consumed by the fan at different PWM percentages. This test was performed with the fan installed in the server and running the leads outside the Nexalus server enclosures. Measurements were performed on two fans and

an average was used. The results of the profiling can be seen in Figure 7 where a cubic polynomial relationship between fan speed and fan power is derived as shown on the graph.

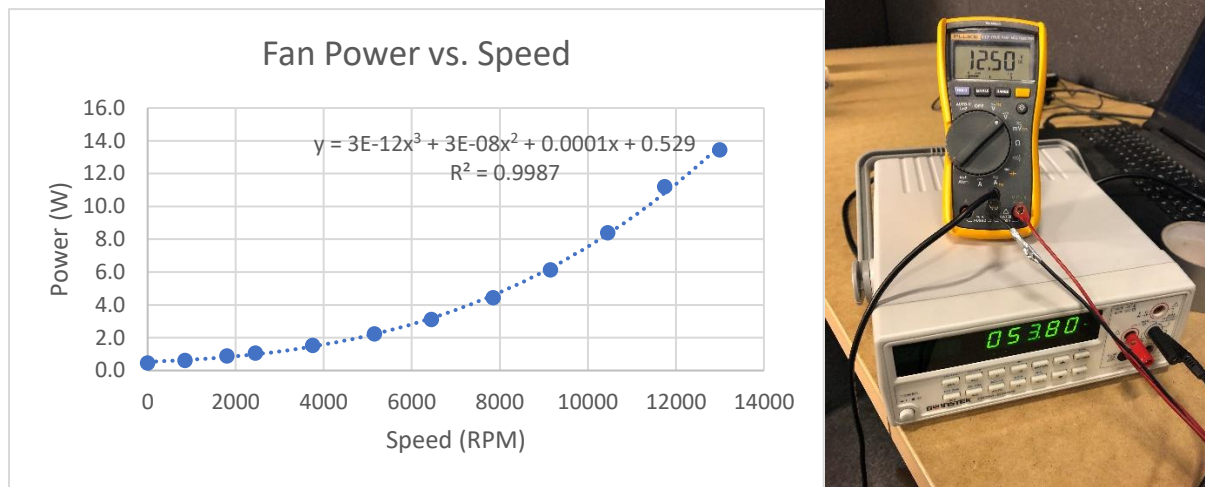


Figure 7: Plot of data showing relationship between server fan speed and power. On the right a picture is shown which was taken during the experiment.

Data collection

All data in the experiment has been collected and stored at the RISE ICE test and demo data center lab using the inhouse RISE data collection chain based on open-source tools. The tools have been employed in several funded projects and details have been published at an Energy Efficient Data Center workshop [2].

Control Methodology

The approach to control of the Nexalus cubby experimental setup was to make a fair comparison with the same server-type under an air-controlled arrangement using the open server wind tunnel. In the wind tunnel, the server fans were operated using a proportional, integral and derivative (PID) controller instead of the server native control to target a fixed central processing unit (CPU) temperature by adjusting the speed of the fans. The details of the server wind tunnel control were recently presented at the IThERM 2020 conference [3]. The servers' air supply temperature in the wind tunnel was controlled by a heater and cooler at the entrance as documented in the paper with the addition of a variable flow rate of the air that maintained a neutral pressure drop across the server. Therefore, three principal control variables were used to assess the air-cooled servers, namely CPU temperature, front of server supply temperature and wind tunnel flow rate to match the servers' flow rates governed by the server fans. A set of results is then created for different digital workloads based on *stress-ng*³ where a percentage workload is demanded.

For the liquid cooled server results, two input controls were created. One to control the CPU temperature as before, and this is based on setting the pump speed for the water circuit that includes all the CPUs as depicted in Figure 8, and the second was the control variable that sets the desired liquid cooling testbed so that the water flow to the CPUs has a set temperature. Three temperature set points have been used,

³ <https://kernel.ubuntu.com/~cking/stress-ng/>

two classed as W4 on the ASHRAE guidelines, namely 30°C and 40°C, and the third classed as W5 at 50°C. The servers in the 1U cubby have the server DIMMs cooled by fans that circulate air over an air to liquid heat exchanger, see Figure 9. The speed of these fans can be set using the OCP Fan Speed Control Interface⁴ and this was not controlled in the experiments present here, but rather fixed to a set speed. The speed selected in the experiments was to bring the temperature range into the same ballpark as reported for the air-cooled server arrangement for low CPU workloads.

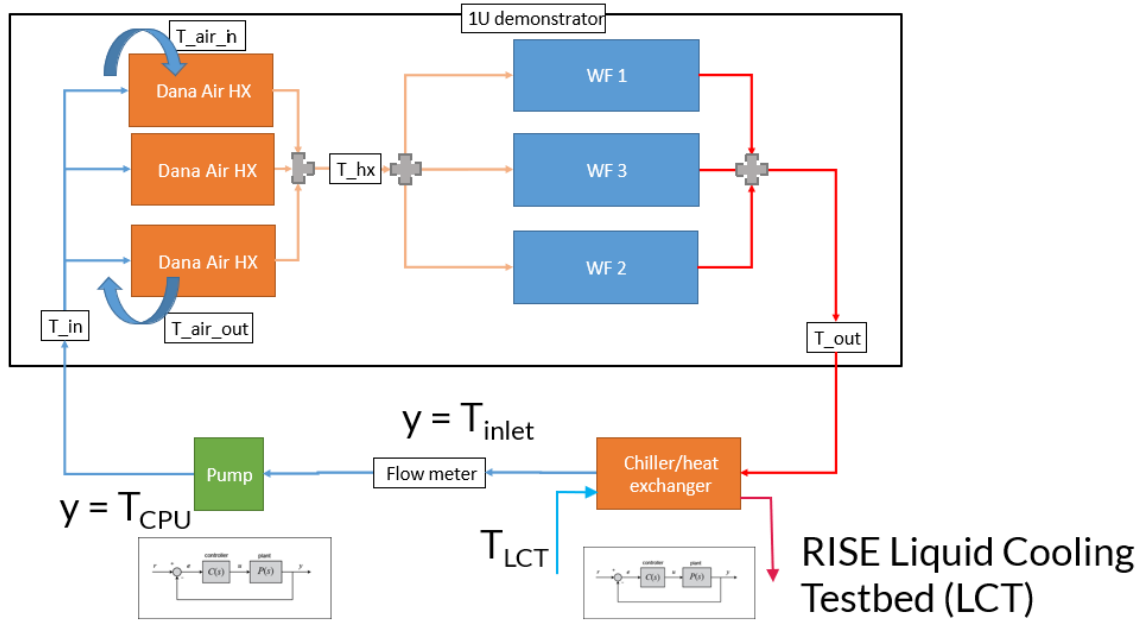


Figure 8: Measurement and control schematic

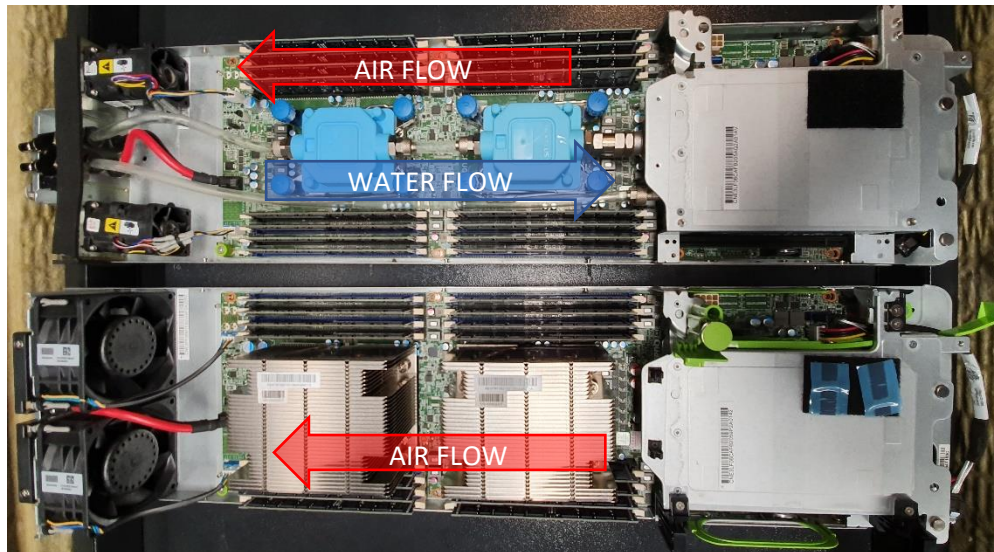


Figure 9: Photo showing the 20U air-cooled OCP server (lower) and the 1U direct-to-chip Nexalus cooled OCP server (upper). Note that the water flow and air flow are in opposite directions as indicated and that there are small fans in the upper server to supply air to the DIMMs.

⁴ <https://www.opencompute.org/documents/facebook-server-fan-speed-control-interface>

Results and Analysis

The Nexalus direct-to-chip solution analysed in this report are retrofitted 20U 2nd generation Open Compute Project Servers with two Intel Xeon E5-2678 v3 2.5GHz 12 core/30MB cache CPUs (Haswell, 22nm, Q3'2014) with 256GB of DDR3-1866 ECC RAM and Mellanox ConnectX-3 EN 10GbE NICs. The motherboards are Quanta Intel V3.1. The result of the Nexalus retrofit is a denser solution with 10U encasements, doubling the number of potential cubbies per rack, with the DIMMs being cooled via recirculation of air over air to liquid heat exchangers with enclosed flow and return paths respectively through the servers and channels at the edges of the enclosure, see Figure 10. The novel server enclosure approach for the DIMM thermal management reduces the need for additional rack level cooling as usually required by direct-to-chip solutions where 25% of the thermal power ends up in the data hall or requires a rear door air to liquid heat exchanger.

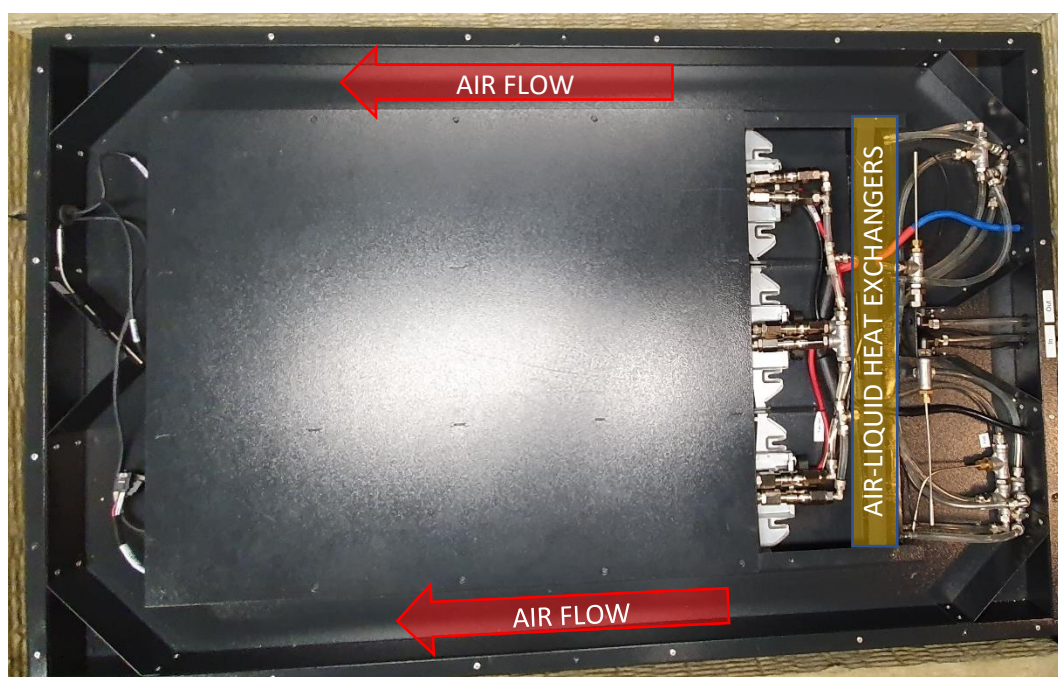


Figure 10: 3 OCP server enclosure showing the water and DC power connection points and the channels for the recirculated air over the air-to-liquid heat exchangers.

The IT workloads are 8%, 50% and 75% based on the number of CPU cores engaged in the workload on each of the 3 OCP servers. Therefore, 50% IT workload would deploy compute activity to half of the cores in each of the 3 OCP servers, 8% is one core per CPU and 75% is 9 cores per CPU. Figure 11 shows how the average CPU operating temperature affects the server thermal power for the different water supply temperatures at the different workloads. As the temperature of the CPUs increases, the server thermal power increases because of the current leakages from the microelectronics. It is interesting to note in Figure 11 that the air-cooled system with an air inlet temperature of 30°C generates a similar current leakage curve and what is clear is that the cooling approach or coolant supply temperature has little effect on the server thermal power. However, the DIMM power consumption and temperatures will be affected by more intensive memory workload applications, such as *prime95*⁵. The higher temperature CPU values

⁵ <https://www.mersenne.org/download/>

are achieved by slowing down the coolant water flow rate and therefore there would be less cooling power required. Figure 12 demonstrates this for the three IT workload scenarios over the range of temperatures for the three different water supply temperatures. As noted from the plots there is a higher cooling overhead in the Nexalus setup than in the air-cooled arrangement, but this is clearly due to the small 10U fans used to recirculate air over the DIMMS since dropping these fans speeds from 50% to 15% shows that the server only cooling power for 30°C air-cooled is like the 30°C cooling water supply temperature and the Nexalus servers warrant DIMM temperature fan control. Note that with the air-cooled arrangement at 30°C supply air the lower average CPU temperatures are not achievable.

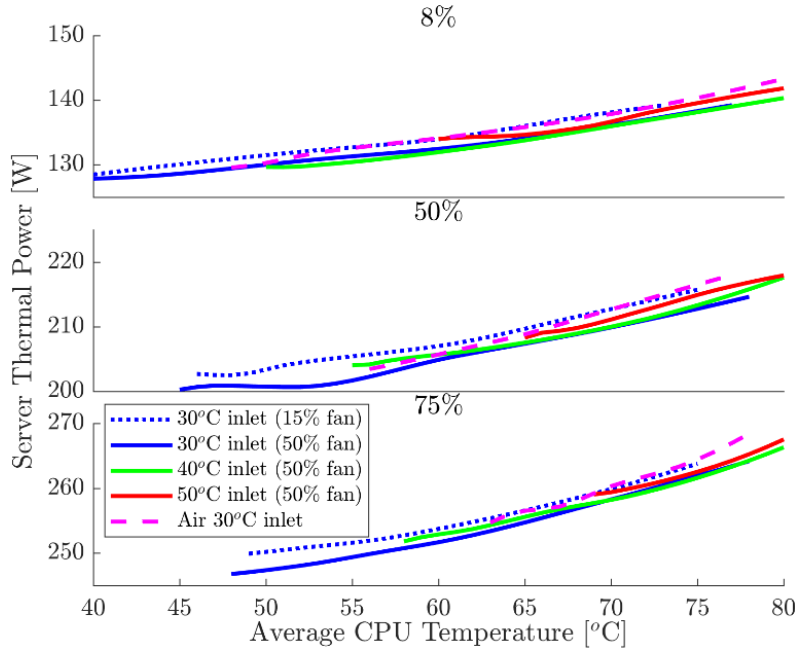


Figure 11: Plots showing the average server thermal power based on the targeted average CPU temperature.

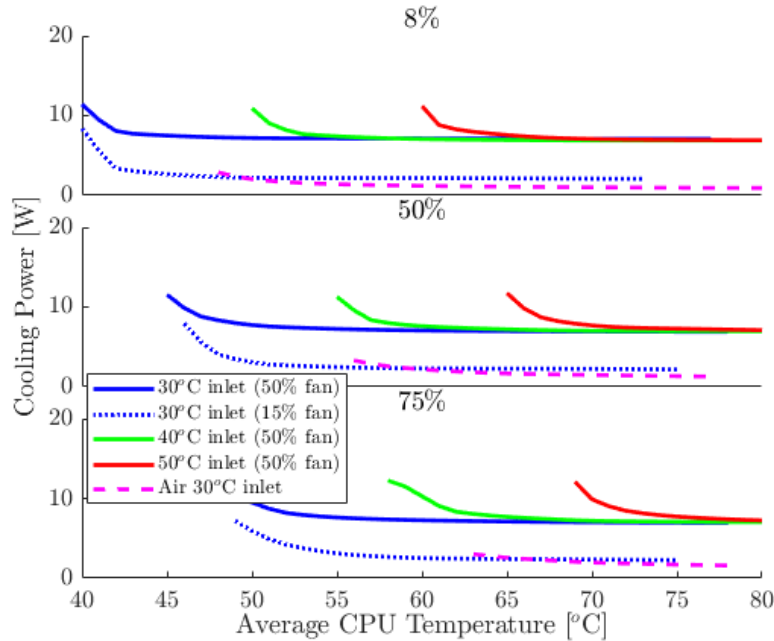


Figure 12: Cooling power consumption (water pump and fans for memory) as a function of the targeted CPU temperature.

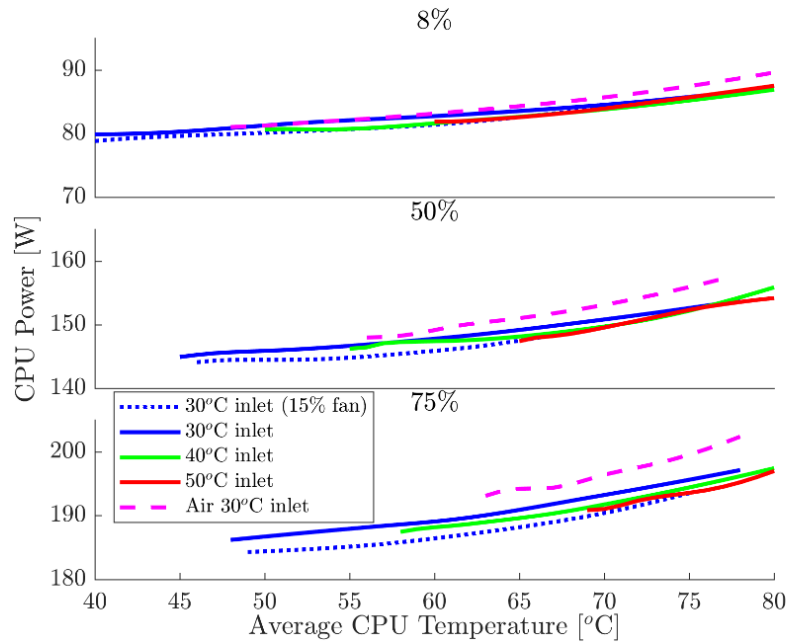


Figure 13: CPU power consumption as a function of the average CPU temperature for the 3 IT workloads.

The obvious next question is how the CPU power varies as a function of the targeted average CPU temperature for the different workloads. This is demonstrated in Figure 13, which shows that over the range of water supply temperatures the current leakages from the CPUs in the Nexalus setup are marginally less than those in the air-cooled servers in the wind tunnel. However, this should not be read that the direct to CPU cooling is performing better than the air-cooled system as these curves should lie on top of each other (for both server cooling methods), this indicates that there is variability in the CPU power draw and there is variability in the IPMI temperatures of the CPU, as these are known to have a certain level of inaccuracy.

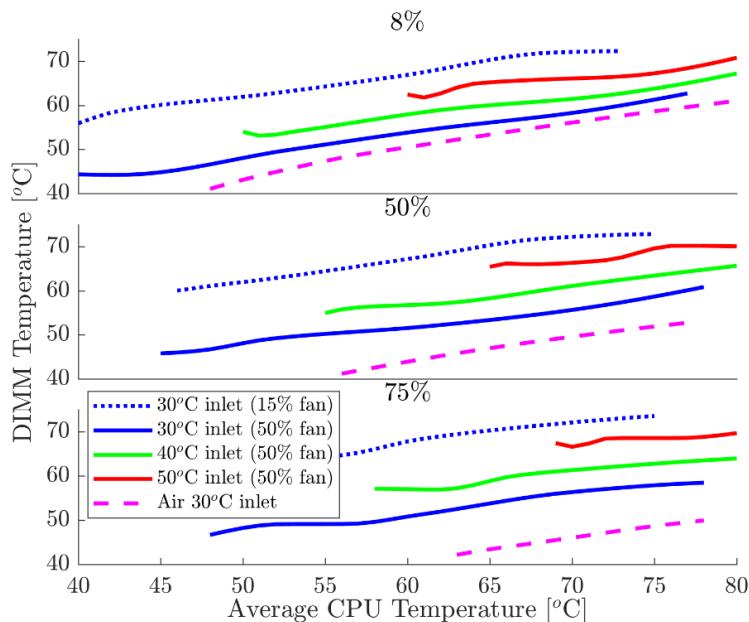


Figure 14: DIMM temperatures as a function of targeted CPU temperatures. Note: DIMM temperatures should stay below 85°C.

In this study, no control strategy is tested the cooling of the DIMMs, so the fans are set at a fixed speed (50%) when sweeping through the targeted CPU temperatures. It is clear however that the water coolant supply temperature and the fan speed setting have an influence on the DIMM temperatures over the range of CPU temperatures as is shown in Figure 14. The plots show that the temperature of the DIMMs run hotter with both the increased water coolant temperature and decrease of the speed of the small fans, as is to be expected. The same trend is observed for the air-cooling servers in the wind tunnel.

Bringing the CPU power consumption together with the cooling (pump and fans) to produce an overall average server power consumption produces similar curves to what were produced for the air-cooled servers in the wind tunnel. In essence there is a minimum consumption of server power at a certain targeted average CPU temperature for each IT workload and coolant supply temperature. In Figure 15 this behaviour is readily seen where a so-called “sweet spot”, a minimum in the power curve at an average CPU temperature, exists for each workload and coolant supply temperature. This sweet spot also exists for the air-cooled servers but is not readily seen at 30°C air supply since CPU temperatures remain too high to see the benefits of lower current leakages at higher server fan speeds.

Figure 16 shows the excess thermal power (that is minus the CPUs) as average CPU temperature increases and there can be seen to be around 5W of difference between the air-cooled and direct-to-chip arrangements at 8% CPU utilisation widening to around 10W at 75%. A combined effect of flow control and DIMM temperature dependent fan control would be expected to reduce the excess thermal power.

These curves can also be plotted with the thermal power and cooling power separated as shown in Figure 17 for the 30°C coolant supply temperature case where the sweet spot is at the combined minimum of heat production and cooling overhead, but as can be seen increased heat production corresponds to a lower cooling power requirement and vice versa.

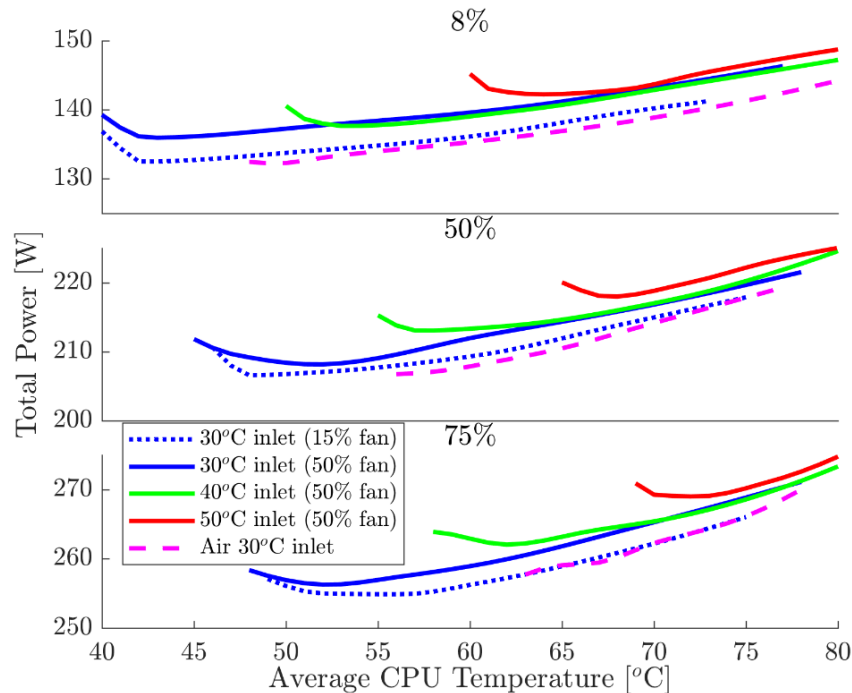


Figure 15: Total power consumed averaged over the three servers in the cubby for the different coolant supply temperatures as the targeted average CPU temperature is varied.

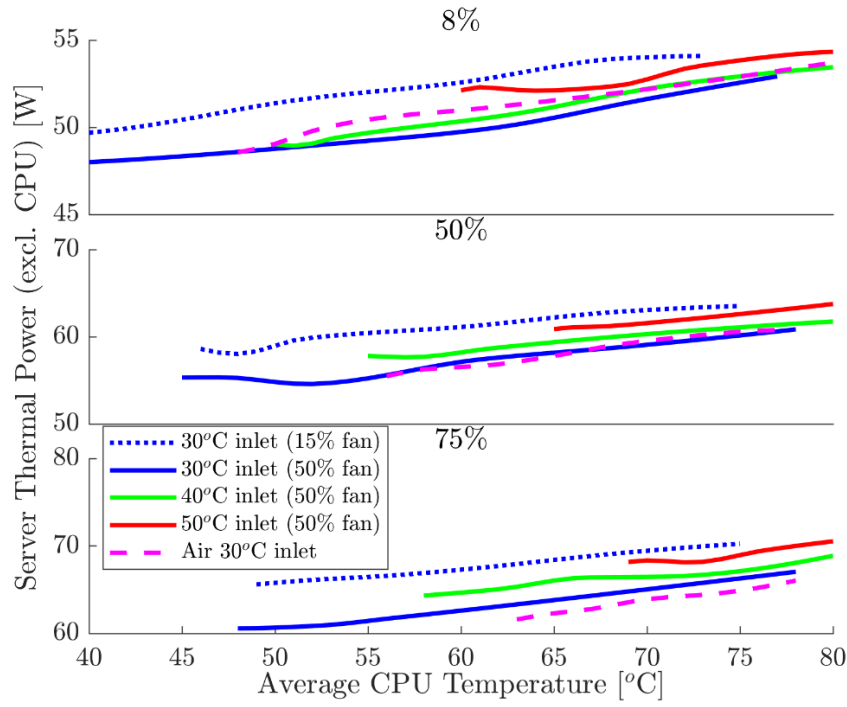


Figure 16: Server thermal power after the CPU thermal output is discounted.

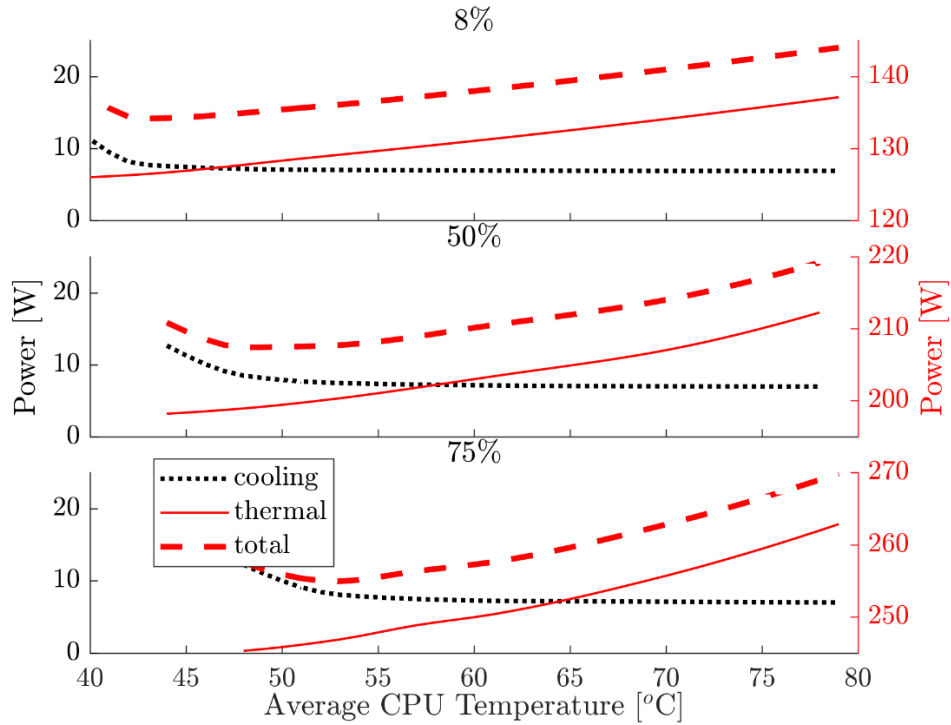


Figure 17: Breakdown of average total power consumption for each server between cooling and thermal when the coolant supply is at 30°C.

Similar curves are also shown in Figure 18 for the higher water coolant supply temperatures of 40°C, shown in the left plot, and 50°C, shown in the right. A consequence of the supply temperature is observed in both Figure 17 and Figure 18, namely that the average CPU temperature is approximately 17°C above the coolant supply temperature, which is why the targeted CPU temperature cannot be lower than the coolant supply temperature plus 17°C, but as can be seen in Figure 15 this difference for the air-cooled setup at 75% workload is nearer 33°C and demonstrates the advantage of the Nexalus direct-to-chip arrangement.

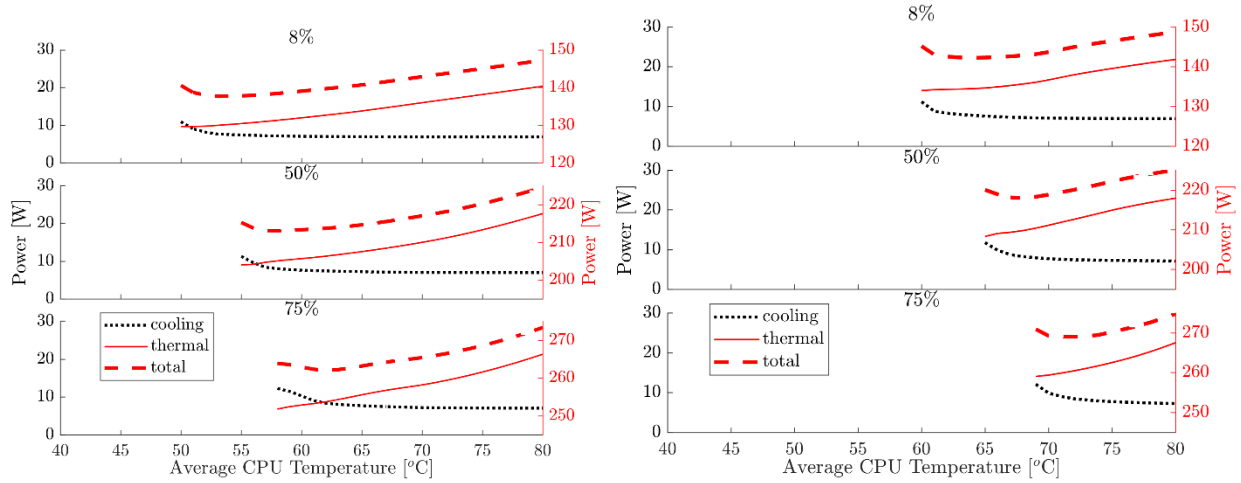


Figure 18: Breakdown of thermal power production and required cooling power overhead as a function of average CPU temperature for 40°C (Left) and 50°C (right).

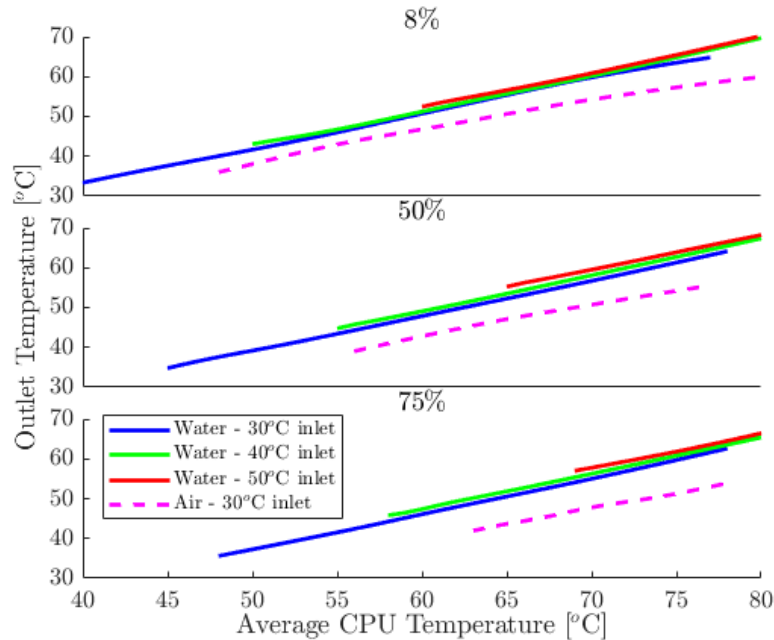


Figure 19: Plots of the return coolant water temperature for the three different workloads and three supply temperatures.

The final plot of the outlet temperature for heat recovery is shown in Figure 19. For the liquid returning to the heat exchanger, it is a measure of the temperature of the water that can be used by waste heat recovery scenarios. Figure 19 shows that it is possible to get 64°C water for heat recovery purposes at a

wide range of IT workloads using a range of coolant supply temperatures, 30°C to 50°C. The corresponding air-cooled hot aisle temperature if channeled could be harvested at around 55°C, but in air there will be temperature losses in any solution that attempts to recover the heat into water for ease of transport.

The data collected from the experimental runs includes coolant flow rate, the ΔT (temperature difference between the return and supply) and the power supplied to the microelectronics and gives a ratio of the thermal power harvested (Liquid power) to the thermal power expected (Chassis thermal power) based on the electrical power supplied to the microelectronics. Table 1 tabulates the heat recovery for the three different workloads and three supply temperatures and it is easily seen that as the supply temperature increases there is a corresponding and expected decrease in recovered heat. For example, at 75% workload it is observed that at each 10°C increase in water coolant supply temperature corresponds in a 2% loss in heat recovered, but this is not at the same CPU temperature, but there is around a 30°C difference between the average CPU temperature and the coolant water supply temperature.

Table 1: Percentage heat recovered for the nine scenarios, three workloads with three coolant supply temperatures.

Inlet Temp	Load	Avg CPU Temp (°C)	Flow (l/min)	Liquid outlet temp (°C)	Blade Power (W)	Liquid Power (W)	Heat Recovery %
30	8	42.5	0.9	35.6	404.4	380.1	94%
30	50	51.6	0.8	40.5	621.9	600.1	97%
30	75	60.8	0.7	46.8	774	761	98%
40	8	53.2	1.0	45.3	410	364	89%
40	50	61.8	0.8	50.6	638	600	94%
40	75	71.0	0.7	57.1	797	769	96%
50	8	64.0	1.0	55.8	423	359	85%
50	50	76.2	0.6	65.0	666	624	94%
50	75	80.7	0.7	67.1	824	777	94%
						Average	93%

A natural question from the analysis in this section is what happens when the CPUs and memory are stressed to 100% by an IT workload, which corresponds to a certain class of high-performance computing workloads. This can be done using the so-called *Prime95* workload tool mentioned earlier, which stresses all the microelectronics. Indicative tests show that the server is operational with a coolant supply temperature of 30°C and 40°C, but not with 50°C and the fans are required to operate near to 100% to keep the DIMM temperature below its maximum of 85°C. If there was a workload scenario that would cause the DIMMs to draw up to their maximum of 120W, the heat from the DIMMs should be revisited in the Nexalus server cooling configurations. Modifications to the air flow routing to the DIMMs and thermal fan control based on the maximum DIMM temperature should be considered to improve DIMM cooling to avoid this threshold.

Conclusion

It is demonstrated that with a well-controlled supply coolant flow rate to the cubby of three OCP servers configured with the Nexalus cooling setup together with accurate monitoring of temperatures and power consumption, sweet spots of operation can be identified for different coolant supply temperatures when the servers are operating at different workloads.

The analysis and comparison against the same servers operating in the RISE ICE test and demo datacenter wind tunnel indicates that waste heat recovery is greatly augmented and made even more feasible with the thermal energy being harvested into water making it more amenable to transportation. It is possible to supply a return coolant water temperature of up to 64°C for all IT workloads including low utilization

whilst maintaining a nearly constant average CPU temperature, achieved by controlling the water flow rate. Comparisons with air-cooled versions of the OCP servers shows that operating the equipment outside the ASHRAE recommended, but in the allowable range only can provide up to 55°C in a confined hot aisle and if transferred into water across an air to liquid heat exchanger would result in temperature losses. An average of 93% of the thermal energy is recovered in the liquid loop from the Nexalus servers for all conditions tested.

There are scenarios of operation where the RAM can be heavily utilised and where the DIMM temperatures can hit their upper limit, since with the Nexalus setup their cooling relies on the circulation of air sealed in the server which is forced and cooled via the 1OU air to liquid heat exchangers. The recirculation of the air in the Nexalus servers offers the benefit of decoupling the DIMM air-cooling from the data hall air and unlike other direct-to-chip solutions no additional rack level cooling is required, however thermal management of the DIMMS in the Nexalus setup should be revisited for improved airflows and fans which could reduce the cooling power to levels commensurate with the air-cooled systems. The Nexalus 1OU form factor of the OCP servers offers an increased compute density, but this analysis recommends that the DIMM cooling strategy for the OCP servers be revisited by Nexalus so that a target of 60°C return coolant temperature is feasible for all IT workloads including scenarios where the CPUs and DIMMS are operating at their peak.

It should be noted that the comparison between the air-cooled versions of the OCP servers with those in the Nexalus arrangement does not consider the infrastructure that provides the air to the OCP servers or the water to the heat exchanger connected to the water loop through the OCP servers. The analysis has therefore been confined to the components that provide the convection within the OCP servers, so that includes the server fans in the air-cooled case and the pump and DIMM fans in the liquid cooled Nexalus arrangement.

References

- [1] ASHRAE Technical Committee, "Thermal guidelines for data processing environments-expanded data center classes and usage guidance," American Society of Heating, Refrigerating and Air-Conditioning Engineers, Atlanta, GA. USA, 2015.
- [2] J. Gustafsson, S. Fredriksson, M. Nilsson-Mäki, D. Olsson, J. Sarkinen, N. H. N. Seyvet, T. Minde and J. Summers, "A demonstration of monitoring and measuring data centers for energy efficiency using opensource tools.," in *Proceedings of the Ninth International Conference on Future Energy Systems (pp. 506-512)*, 2018.
- [3] J. Sarkinen, R. Brännvall, J. Gustafsson and J. Summers, "Experimental Analysis of Server Fan Control Strategies for Improved Data Center Air-based," in *19th IEEE Intersociety Conference on Thermal and Thermomechanical Phenomena in Electronic Systems (ITherm) (pp. 341-349)*, IEEE, 2020.